Recovery of rare earths from waste cathode ray tube (crt) phosphor powder by selective sulfation roasting and water leaching

Mehmet Ali Recai Önal, Koen Binnemans

PII: S0304-386X(18)30522-X
DOI: https://doi.org/10.1016/j.hydromet.2018.11.005
Reference: HYDROM 4937

To appear in: *Hydrometallurgy*

Received date: 16 July 2018
Revised date: 1 October 2018
Accepted date: 17 November 2018

Please cite this article as: Mehmet Ali Recai Önal, Koen Binnemans , Recovery of rare earths from waste cathode ray tube (crt) phosphor powder by selective sulfation roasting and water leaching. Hydrom (2018), https://doi.org/10.1016/j.hydromet.2018.11.005

Manuscript for: *Hydrometallurgy*

Recovery of Rare Earths from Waste Cathode Ray Tube (CRT) Phosphor Powder by Selective Sulfation Roasting and Water Leaching

Mehmet Ali Recai Önal, Koen Binnemans*

KU Leuven, Department of Chemistry, Celestijnenlaan 200F box 2404, B-3001 Leuven, Belgium

*Corresponding author. Tel.: +32 16327446

E-mail address: Koen.Binnemans@kuleuven.be

Abstract

Until recently, most displays, such as television and computer screens, were based on cathode ray tubes (CRTs). With the introduction of new types of displays including liquid crystal displays, CRTs have been widely replaced, leading to a gradual build-up of hazardous CRT powder waste. In this paper, a new approach is introduced where the valuable rare-earth elements (REEs) (i.e. yttrium and europium) in the powder are selectively recovered, leaving behind a zinc-rich residue and glass for further recycling. The main rare-earth compound in the waste powder is $Y_2O_2S:Eu^{3+}$ (YOS). The fine-grained CRT powder was mixed with zinc sulfate monohydrate ($ZnSO_4 \cdot H_2O$) and roasted at 600-900 °C for short periods of time. In this way, $Y_2O_2S:Eu^{3+}$ was transformed into water-soluble rare-earth sulfates. Meanwhile, ZnS underwent a two-stage reaction with $ZnSO_4 \cdot H_2O$, where first a partially water-soluble intermediate ($ZnO \cdot 2ZnSO_4$) and then the water-insoluble ZnO was formed. Addition of a sufficient amount of $ZnSO_4 \cdot H_2O$ ensured the recovery of ≥ 95% of the rare earths in a subsequent water leaching step, but there was also co-dissolution of about 5% of the total amount of zinc present. Several purification methods were tested and compared to separate the REEs from the zinc impurity in the solutions. In addition to the conventional precipitation methods with sulfides and oxalic acid, a novel liquid-liquid exchange reaction between REE-containing leachate and zinc-loaded Versatic Acid 10 was tested. Finally, a complete flow sheet is proposed for the (almost complete) valorization of REEs as well as the total zinc present.

Keywords: CRT phosphor; roasting; water leaching; rare earths; zinc; Versatic acid.

1. Introduction

Cathode ray tubes (CRTs) have been used for several decades in numerous display applications including TVs, computer screens, oscilloscopes and radar-receiving equipment. The success of CRTs was the result of their mature technology, low price, high reliability and long lifetime. However, since the year 2000 the global demand for CRTs has sharply declined and their annual production has surpassed their annual demand (Yu-Gong et al., 2016). The reason behind this decline is the shift in the major CRT market: display technologies. With the introduction of liquid crystal display (LCD) and light emitting diode (LED) technologies, the problems associated with CRTs can be overcome: screen size restriction, heavy weight and large volume, heat production, generation of high-energy radiation and energy-inefficiency. As a consequence, the disposal of old CRT-containing waste electrical and electronic equipment (WEEE) gradually gained momentum in the recent years. Prior to 2012, the discarded television and computer screens containing CRTs corresponded to 22 wt.% of the total WEEE in Europe and 58 wt.% of the total regulated e-waste in the United States, respectively, while in China ca. 2400 million CRT screens were disposed of between 2001 and 2013 (Tian et al., 2016; Xu et al., 2013). In Europe, 50,000–150,000 tons of end-of-life CRT material is collected every year while the global waste generation was reported as 6.3 Mt in 2014 (Singh et al., 2016). This continuous pile-up of the waste CRT material requires development of more efficient, environmentally-friendly and economical flow sheets. In earlier periods, after removal of electronic circuits containing valuable metals such as gold and copper, the waste CRT materials were simply landfilled. Because CRT wastes contain hazardous elements such as lead and cadmium, strict regulations have been issued over the years in several countries including the US, the European Union and Japan for CRT waste management (Herat, 2008). These regulations have resulted in a

more effective collection of different types of waste which are therefore now readily available for recycling treatments. Several innovative attempts for partial or complete recycling of the waste CRT material have been proposed in the literature and these attempts were critically evaluated elsewhere (Ciftci and Cicek, 2017; De Michelis et al., 2011; Dexpert-Ghys et al., 2009; Grause et al., 2016; Herat, 2008; Innocenzi et al., 2013a, 2013b; Meng et al., 2016; Okada and Yonezawa, 2014; Resende and Morais, 2010, 2015; Strauss et al., 2017; Tian et al., 2016; Van Den Bogaert et al., 2015; Xu et al., 2013; Yao et al., 2016; Yin et al., 2016; Yu-Gong et al., 2016).

Especially after the so-called rare-earth supply crisis in 2009, efforts have been given for the recycling of the rare-earth elements (REEs) present in secondary raw materials such as waste NdFeB magnets, nickel metal hydride batteries and lamp phosphors (Binnemans et al., 2013; Innocenzi et al., 2014, 2013b, 2013a, Önal et al., 2017a, 2017b, 2015, Tunsu et al., 2016, 2014; Van Loy et al., 2017). CRTs are a rich source of rare earths too. The screen of a CRT device contains on average 7 g of luminescent powder. The rare earths are present as yttrium and europium in the red phosphor $Y_2O_2S:Eu^{3+}$ (YOS). For the green and blue colors, ZnS-based phosphors doped with silver and copper are used. To recover the valuable REEs from the CRT powder, most of the proposed methods are partially or completely based on hydrometallurgical methods involving dissolution in strong acids or bases (Dexpert-Ghys et al., 2009; Innocenzi et al., 2013a; Resende and Morais, 2015, 2010; Tian et al., 2016; Yin et al., 2016). However, dissolution of the sulfide compounds generally requires the addition of an oxidizing agent to achieve high leaching efficiencies (> 90%). The most commonly used acid and the most commonly used oxidizing agent are sulfuric acid (H_2SO_4) and hydrogen peroxide (H_2O_2), respectively. Innocenzi et al. (2017) showed that the addition of H_2O_2 improved the H_2SO_4

leaching rate of a CRT powder and decreased the activation energy of the process (Innocenzi et al., 2017). A problem with the dissolution of sulfide compounds in strong acids is the formation of highly toxic H_2S gas. Dissolution in the more expensive nitric acid (HNO_3) causes the additional formation of toxic NO_X gases. Only the combination of 4 M HCl and 1 M H_2O_2 was found to largely eliminate the formation of H_2S gas (Tian et al., 2016). However, the combination of HCl and H_2O_2 gave lower leaching efficiencies for yttrium and europium, with slower dissolution kinetics than those observed for other mineral acids under the same conditions.

Another important issue that must be considered is the selectivity for REEs dissolution against several other metals, and especially towards the main constituent zinc (accounting for circa 30 wt.% of the CRT powder). In the case of acid treatment of the CRTs, the acid and the oxidizing agent are effective to a certain extent for dissolution of both ZnS and $Y_2O_2S{:}Eu^{3+}$. In a recent study, direct acid leaching of a CRT powder with diluted sulfuric acid (i.e. ≤ 1 mol L^{-1}) resulted in less 10% Y, Eu and Zn and 50% Cd dissolution. However, with combination of H_2O_2, these leaching efficiencies could be increased up to ~95% for Y and Eu, 20% for Zn and 80% for Cd, giving some degree of selectivity (Miskufova et al., 2018). Innocenzi et al. (2013) studied the oxidative sulfuric acid leaching followed by Zn removal with Na_2S addition to reform ZnS in the leachate (Innocenzi et al., 2013a). However, 20-25% of the dissolved yttrium and europium were lost via co-precipitation. The remaining REEs were then precipitated by addition of oxalic acid, yielding a high-purity mixed REE oxide after calcination. Despite being present only in minor quantities, several minor elements present in the CRT powder co-dissolved during the acid leaching step and most of them, including Al, Fe, Ca, Mg, Cd and S, also reported to the mixed REE oxide. On the other hand, Yin et al. (2016) claimed to remove $\geq 98\%$ of the impurities

including most of the ZnS, glass portion and aluminum flakes from the CRT powder, but the details of this pretreatment are not given (Yin et al., 2016). After oxidative HCl leaching of the enriched powder, they obtained a high-purity yttrium oxide (> 99.5 wt.%) by directly applying oxalate precipitation for 12 to 15 h. The pH of the acidic leachate was controlled at 1.8 to 2.0 by addition of ammonia. In another study, selective removal of ZnS was achieved by oxidative alkali leaching of the CRT powder with a mixed solution of NaOCl and NaOH (Dexpert-Ghys et al., 2009). The residue containing $Y_2O_2S:Eu^{3+}$ and glass particles was then thermally treated to produce the red fluorescent lamp phosphor $Y_2O_3:Eu^{3+}$ (YOX). However, the efficiency of the process was low because the process temperatures (e.g. 1200 °C) induced the formation of compounds other than YOX, e.g. complex yttrium-europium silicates such as $(Y_{1-x}Eu_x)_{4.67}(SiO_4)_3O$. In a recent study, subcritical water extraction (SWE) was performed on a CRT powder with sulfuric acid. At 150 °C, under 10^6 Pa pressure and with 0.75 M acid concentration, complete leaching of yttrium and europium was achieved with 36% Pb and 9.4% Zn co-dissolution (Lin et al., 2018). It is also important to note that recycling of the consumed reagents in the above-mentioned methods was limited or even absent. Pyrometallurgical pre-treatments (e.g. alkali roasting) were found to improve the leaching efficiencies of REEs from hard-to-dissolve mineral phases such as the green phosphors in fluorescent lamps (Ippolito et al., 2017, 2016; Zhang et al., 2013). In this paper, a new combined pyrometallurgical and hydrometallurgical flow sheet was developed to avoid the use of strong acids or bases. The formation of H_2S was prevented so that there was no need for using an oxidizing agent. The process consisted of several stages. First, the fine-sized CRT powder is mixed with zinc sulfate monohydrate ($ZnSO_4 \cdot H_2O$ or ZSMH). Next, the mixture is roasted to convert $Y_2O_2S:Eu^{3+}$ into sulfates. Finally, europium and yttrium are dissolved by water leaching. The total zinc

dissolution was kept as low as possible to obtain a highly pure REE product. High roasting temperatures were avoided to prevent the formation of complex zinc silicates such as willemite, which would be difficult to subsequently dissolve zinc from the zinc-rich leaching residue. ZSMH was chosen since it does not contaminate the system with other metals and it can be recovered by electrolysis as metallic zinc.

2. Materials and methods

2.1. Chemicals

$ZnSO_4 \cdot H_2O$ (ZSMH) (purified, > 98%) was obtained from VWR (Haasrode, Belgium). Ethylene glycol (for analysis, 99.91%) was ordered from Acros Organics, (Geel, Belgium). $Na_2S \cdot 9H_2O$ (ACS reagent, ≥ 98.0%,) ZnO (> 99%) and oxalic acid (> 99.0%) were obtained from Sigma–Aldrich (Diegem, Belgium). Versatic Acid 10 was purchased from Resolution Europe B.V. (the Netherlands). The CRT powder sample was supplied by the WEEE collection and recycling company Relight SRL (Rho, Italy). As the received batch contained coarse pieces of glass, it was homogenized by grinding with a disc mill (Fritsch Pulverisette 13) and the whole sample was sieved to get a particle size of < 500 µm.

2.2. Materials Characterization

The semi-quantitative chemical characterization of the homogenized CRT powder (about 7 g) was performed by a Bruker S8 Tiger 4K wavelength dispersive X-ray fluorescence (WD-XRF) spectrometer. The fully quantitative composition of the powder for zinc, yttrium and europium was determined by an Optima 8300 inductively coupled plasma optical emission spectrometer (ICP-OES). For that purpose, an open-air digestion was performed based on the methodology in

reference (Lin et al., 2018). Two samples, each with about 0.25 g of the CRT powder, were mixed gradually with HCl (37%), HNO_3 (65%), H_2SO_4 (98%), H_2O_2 (30%) and demineralized water in a volume ratio of 3:2:0.5:2:5, respectively. The mixtures were stirred on a hot plate at 60 °C for 8 h and left for open-air digestion over the course of 6 days. The mixtures were then completely transferred to volumetric flasks where only some glass pieces were visible. After filtration through a syringe filter with 0.45 µm pore size, the solutions were further diluted accordingly before the analysis. The obtained results for zinc, yttrium and europium were comparable to the analysis of the supplier. Mineralogical analysis was performed by a Bruker D2 PHASER XRD with Cu-Kα X-ray radiation (30 kV; 10 mA). The step size increment was 0.02 (2θ) with 0.06 second/step. The raw data were processed both with the X'pert HighScore Plus PANalytical and EVA software with the ICDD database. A Phillips XL30 FEG model scanning electron microscope (SEM) was used to better understand the complete mineralogy of the sample. Chemical analysis of the aqueous leachates and the mixed REE oxide dissolved in an HNO_3:HCl:H_2O (1:1:0.5 volume ratio) acid mixture was performed by ICP-OES. The solid residue obtained under the selected optimum conditions and the mixed REE oxide were additionally analyzed by WD-XRF.

2.3. Experimental Set-up and Procedure

For roasting experiments, 30 mL cylindrical alumina crucibles were used. A CRT powder sample of about 1 g (< 500 µm) and 1–3 g of $ZnSO_4 \cdot H_2O$ (ZSMH) were mixed with a spoon giving a 1–3 ZSMH/CRT ratio. The homogenized mixture was then roasted in a pre-heated muffle furnace at selected temperatures between 600 and 900 °C for 15 to 180 min. At the end of the roasting step, the crucible was removed from the furnace and left for cooling open to the air.

Since there was no paste formation or sintering, the calcine could easily be pulverized and poured into a polyethylene bottle along with 10, 25 or 50 mL of demineralized water, giving a CRT concentration of 100, 40 or 20 g L^{-1}, respectively. In some leaching experiments, the water was replaced partially or completely by ethylene glycol while maintaining the CRT concentration at 20 or 40 g L^{-1}. To observe the mass change and to ensure that no solid was left in the crucibles, sample masses were measured after each step. The sludge in the polyethylene bottles was then placed in a unidirectional horizontal shaker (Gerhardt Laboshake) and stirred at 200 rpm for 1 to 96 h at 25 °C.

After water leaching, the sludge was filtered twice through a syringe filter with 0.45 µm pore size. The leachate was analyzed in triplicate by ICP-OES for calculation of the leaching efficiencies. Calculated relative standard deviations (RSD) in the metal concentrations for all reported results were ≤ 2%. For the replicability of the experimental results, the same experiment was repeated with the optimum conditions several times while producing a stock leach solution. The standard deviation in the leaching efficiencies of Y, Eu and Zn in 10 of these experiments was found as 0.51%, 0.91% and 0.59%, respectively. Solid samples for XRD and WD-XRF analyses were recovered by filtering the sludge under vacuum through a Buchner funnel with Whatman-grade 542 filter paper. The filter cake was subsequently washed with ca. 500 mL of demineralized water to completely remove any entrapped leachate and then dried overnight at 60 °C. The pH of the leachate was measured with a Pt–Ag/AgCl electrode that was saturated with a 3 M KCl solution (WTW Sentix 81). The leaching efficiencies of the Y and Eu were calculated by using Eq. (1). Since both the CRT powder and added ZSMH contained Zn, the Zn source of the leachate was not distinguishable. Hence, the total Zn percentage leaching was calculated based on Eq. (2) while the total Zn amount entering the system, Zn_{total}, was calculated by Eq. (3).

$$\text{REE leaching percentage (\%)} = 100 \text{ x } \frac{\text{REE in solution (g)}}{\text{REE in CRT powder (g)}} \quad (1)$$

$$\text{Zn leaching percentage (\%)} = 100 \text{ x } \frac{\text{Zn in solution (g)}}{\text{Zn}_{\text{total}} \text{ (g)}} \quad (2)$$

$$\text{Zn}_{\text{total}} \text{ (g)} = (\text{Zn in CRT powder (g)}) + (\text{Zn in } ZnSO_4 \cdot H_2O \text{ (g)}) \quad (3)$$

After optimization of the roasting and leaching parameters, a set of conditions was selected as optimum and a large batch was prepared for further purification treatments. In sulfide or oxalate precipitation experiments, a pre-determined amount of $Na_2S \cdot 9H_2O$ or oxalic acid, as specified in the results and discussion section, was directly added to 10 mL of leachate. After rapid addition of these reagents, the mixtures were stirred at 700 rpm on a magnetic stirrer at room temperature for 1 h. The solution was then separated by a syringe filter and analyzed by ICP-OES for its chemical composition. The precipitation (%) of any metal *M* was calculated based on Eq. (4) for both treatments.

$$\text{Precipitation percentage (\%)} = 100 \times \left(\frac{\text{M in input leachate (g)} - \text{M in filtrate (g)}}{\text{M in input leachate (g)}}\right) \quad (4)$$

As an alternative approach, selective extraction of yttrium and europium from the zinc-containing aqueous leachate to an organic phase was studied by an exchange reaction with Versatic Acid 10 (VA). First, a stock organic solution was prepared where a pre-determined amount of pure ZnO was dissolved in concentrated VA. Then, the zinc-loaded VA was brought

in contact with the aqueous leachate with a volume ratio of 0.10-10 and stirred at 2000 rpm for 1 or 24 h at 30 °C. After each experiment, the mixture was centrifuged at 5000 rpm for 10 min and the aqueous solution was drained by the help of a syringe before ICP-OES analysis. The percentage extraction of yttrium or europium to the VA phase was calculated by Eq. (5) where $REE_{aq,in}$ and $REE_{aq,out}$ refer to the amount of REE (mg) in the input and output leachate after liquid-liquid extraction, respectively. The percentage extraction of zinc in the initial VA solution to the aqueous leachate was calculated through Eq. (6) where $Zn_{or,in}$, $Zn_{aq,in}$ and $Zn_{aq,out}$ refer to the amount of Zn (mg) in the initial VA, the input and output leachate, respectively.

$$\text{REE extraction percentage to the organic phase } (\%) = 100 \times \left(\frac{REE_{aq,\,in} - REE_{aq,\,out}}{REE_{aq,\,in}}\right) \quad (5)$$

$$\text{Zn extraction percentage to the aqueous phase } (\%) = 100\text{-}100 \times \left(\frac{Zn_{or,\,in} - \left(Zn_{aq,\,out} - Zn_{aq,\,in}\right)}{Zn_{or,\,in}}\right) \quad (6)$$

3. Results and discussion

3.1. Characterization of Materials

The chemical composition of the homogenized CRT powder measured by both quantitative ICP-OES and semi-quantitative WD-XRF is given in Table 1 where the balance is oxygen, carbon and quite possibly sodium. In accordance with the XRD pattern in Fig. 1 and the semi-quantitative SEM-EDX analysis (not reported here), the mineralogical composition of the powder can be approximated as 20-25 wt.% $Y_2O_2S{:}Eu^{3+}$, 45-48 wt.% zinc sulfide (ZnS) and 2-3 wt.% metallic aluminum flakes. Although it cannot be seen in Fig. 1 due to its amorphous nature,

the remaining 20-25 wt.% of the CRT powder consisted of glass particles which can contain some Al and Na as well.

Table 1 Chemical composition of the CRT powder used in the study based on ICP-OES and WD-XRF methods.

Method	ICP-OES	WD-XRF	Method	WD-XRF
Element	wt.%		Element	wt.%
Y	15.1 ± 0.5	19.8	Mg	0.07
Eu	0.92 ± 0.2	2.09	Fe	0.14
Zn	29.7 ± 0.5	32.5	Cd	0.20
S		14.5	Zr	0.35
Si		2.83	Co	0.12
Al		2.70	Ba	1.96
Pb		2.98	Nb	0.05
K		0.97	Ti	0.04
Ni		0.22	Cr	0.02
Ca		0.19	Cu	0.02
Sr		1.89	Total	83.6

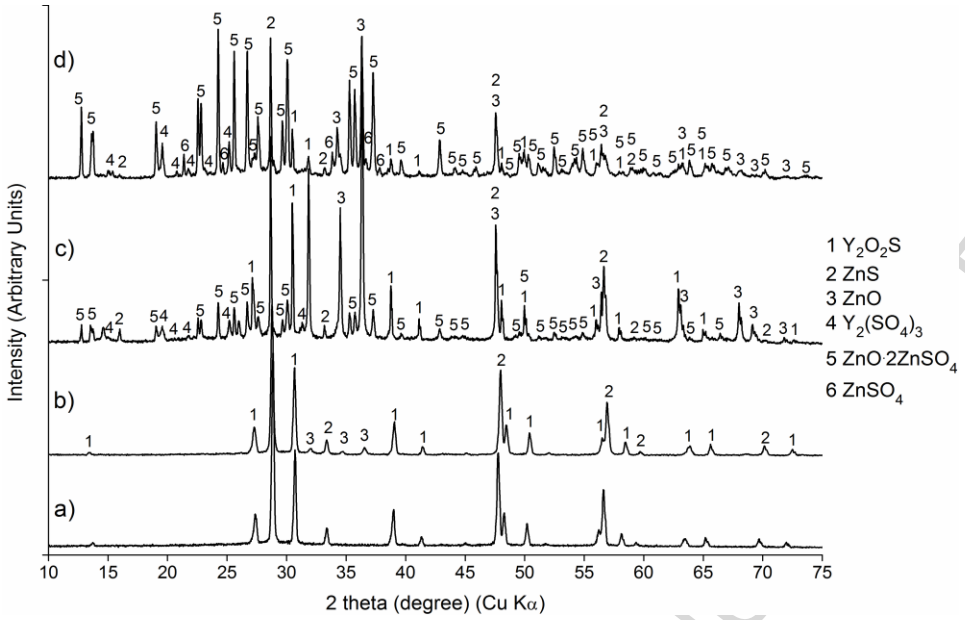

Fig. 1. XRD patterns of the a) starting homogenized CRT powder and the calcines obtained after roasting at 600 °C for 2 h with a ZSMH/CRT ratio of b) 0, c) 1 or d) 3.

3.2. Preliminary Tests and Proof of Concept

The thermal behavior of the binary $ZnSO_4$–ZnS system in an inert atmosphere with a constant heating rate of 6 °C min^{-1} is described in detail in the literature (Malinowski and Malinowska, 1994). Although there are significant differences with our study including particle size, heating medium and profile, use of anhydrous $ZnSO_4$, and presence of other compounds (e.g. $Y_2O_2S:Eu^{3+}$), this study is useful in the sense of reactions between these two compounds that can be observed in our system as well.

Accordingly, up to a $ZnSO_4$:ZnS molar ratio of 3:1, the process consists of two consecutive stages. The first stage starts at about 520 °C. Here, three interrelated reactions, shown in Eqs. (7)-(9), occur giving the overall reaction in Eq. (10). This stage is based on oxidation of ZnS directly to ZnO via Eq. (8), where O_2 is driven from the thermal decomposition of $ZnSO_4$ to an

intermediate complex via Eq. (7). This results in gradual decomposition of $ZnSO_4$ which is further consumed by part of the newly formed ZnO to once again give the complex intermediate via Eq. (9). Hence, the final product of the first stage is the complex intermediate that is responsible for total consumption of free $ZnSO_4$.

$$3\ ZnSO_4 \rightarrow ZnO{\cdot}2ZnSO_4 + SO_2 + 1/2\ O_2 \quad (7)$$

$$ZnS + 3/2\ O_2 \rightarrow ZnO + SO_2 \quad (8)$$

$$ZnO + 2\ ZnSO_4 \rightarrow ZnO{\cdot}2ZnSO_4 \quad (9)$$

$$11\ ZnSO_4 + ZnS \rightarrow 4\ (ZnO{\cdot}2ZnSO_4) + 4\ SO_2 \quad (10)$$

Although the initiation temperature of the second stage is ca. 600 °C, its actual value depends on the $ZnSO_4$:ZnS molar ratio which increases with increasing ratios (Malinowski and Malinowska, 1994). Here, the newly formed intermediate complex starts to decompose to give ZnO via Eq. (11) where the produced O_2 molecule is consumed by the remaining ZnS for its oxidation via Eq. (12) giving the overall reaction in Eq. (13). It is worth to note that the oxidation rate of ZnS with this process is a few times higher than its oxidation by air.

$$ZnO{\cdot}2ZnSO_4 \rightarrow 3\ ZnO + 2\ SO_2 + O_2 \quad (11)$$

$$ZnS + 3/2\ O_2 \rightarrow ZnO + SO_2 \quad (12)$$

$$3\ (ZnO{\cdot}2ZnSO_4) + 2\ ZnS \rightarrow 11\ ZnO + 8\ SO_2 \quad (13)$$

Hence, the overall balanced reaction of the whole process can be summarized by Eq. (14), with the final products being only ZnO and SO_2 gas. It is worth to note that the produced SO_2 can be

captured and used for sulfuric acid production by one of the proposed methods in (Roy and Sardar, 2015). Although there are industrial examples for such practices during roasting or smelting of sulfide minerals (King et al., 2013), further studies are needed to evaluate this option in our particular flow sheet.

$$ZnS + 3\,ZnSO_4 \rightarrow 4\,ZnO + 4\,SO_2 \quad (14)$$

The second stage and thus the whole process ends when all the ZnS is completely oxidized or when the intermediate complex is completely decomposed. Which of the two processes happens first is dependent on the $ZnSO_4$:ZnS molar ratio. In case this ratio exceeds 3:1, a third successive stage appears, which is a continuation of Eq. (11). The complete decomposition of $ZnO{\cdot}2ZnSO_4$ to ZnO was reported to occur at temperatures between 775 and 800 °C (Moezzi et al., 2013). Contrary to the detailed explanation for the case of ZnS, to the best of our knowledge, no literature is available on the thermal interactions between $Y_2O_2S{:}Eu^{3+}$ and $ZnSO_4$. Hence, preliminary tests were carried out to get insight in the behavior of $Y_2O_2S{:}Eu^{3+}$ during roasting with varying amounts of ZSMH added at two different temperatures. The XRD patterns of the calcines are given in Figs. 1 and 2 for the respective temperatures. In the absence of ZSMH, the CRT powder is simply oxidized in air, as will be discussed later (*vide infra*). At 600 °C, the starting microstructure remained to a large extent intact with a small quantity of ZnO formed by air oxidation, as described by Eq. (12) (Fig. 1(b)). With the ZSMH/CRT ratio of 1, the major peaks of ZnO, ZnS and $Y_2O_2S{:}Eu^{3+}$ dominated the calcine, with minor peaks of the intermediate complex, as well as newly formed $Y_2(SO_4)_3$ (Fig. 2(c)). As the amount of ZSMH was tripled, the peaks for $ZnO{\cdot}2ZnSO_4$ became more visible, but the peaks of ZnS and the excess anhydrous zinc

sulfate were still present (Fig. 2(d)). This means that the two-stage mechanism explained in Eqs. (7)-(14) was still on-going and the reaction kinetics were rather slow at 600 °C. Meanwhile, a certain portion of the $Y_2O_2S:Eu^{3+}$ remained still intact, although the peaks of $Y_2(SO_4)_3$ were intensified compared to the case of the ZSMH/CRT ratio of 1. It is also worth mentioning that no intermediate REE phase was detected between these two phases.

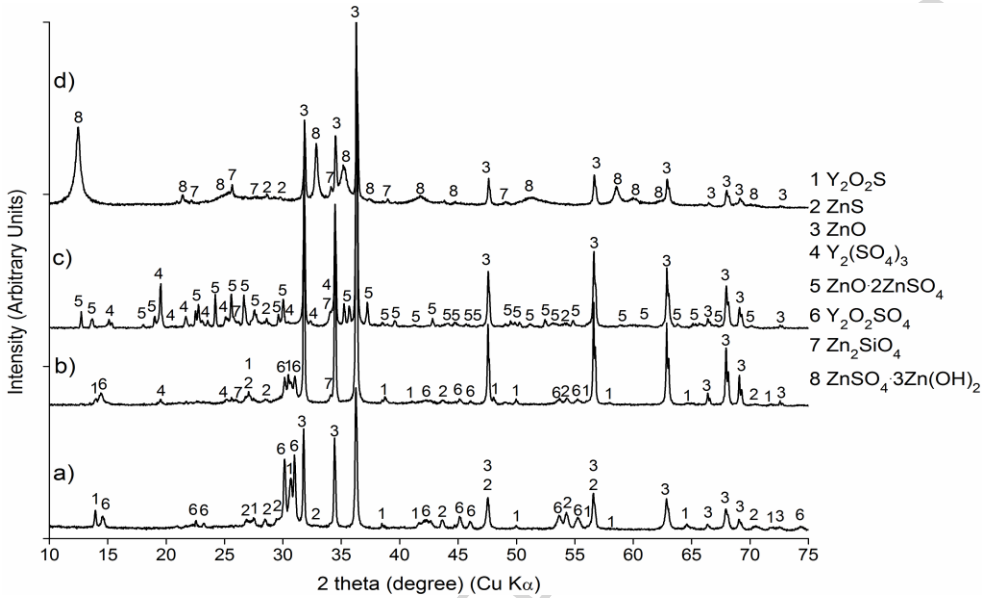

Fig. 2. XRD patterns of the calcines obtained after roasting at 700 °C for 2 h with a ZSMH/CRT ratio of a) 0, b) 1, c) 3 and d) the leach residue obtained after water leaching of the calcine (c) (leaching conditions: 20 g L^{-1} CRT concentration for 24 h at 25 °C).

When the roasting was conducted at 700 °C, the absence of ZSMH resulted in more air oxidation of ZnS, so that ZnO peaks already dominated the calcine (Fig. 2(a)). Meanwhile, $Y_2O_2S:Eu^{3+}$ was partially transformed to give a new phase, yttrium oxide sulfate, doped with Eu^{3+} ($Y_2O_2SO_4:Eu^{3+}$). In agreement with literature data (Dexpert-Ghys et al., 2009), the air oxidation of $Y_2O_2S:Eu^{3+}$ forms this new intermediate, before $Y_2O_3:Eu^{3+}$ is formed. With a ZSMH/CRT ratio of 1, small $Y_2(SO_4)_3$ peaks also emerged while no peaks could be detected for $ZnO{\cdot}2ZnSO_4$

or $ZnSO_4$ (Fig. 2(b)). This means that addition of 1 g of ZSMH per gram of CRT powder was not enough to transform all $Y_2O_2S:Eu^{3+}$ quantitatively into $Y_2(SO_4)_3:Eu^{3+}$. Upon the addition of a ZSMH/CRT ratio of 3, all the peaks of $Y_2O_2S:Eu^{3+}$ disappeared and were replaced by peaks of $Y_2(SO_4)_3$ (Fig. 2(c)). Meanwhile, Zn was mainly present in the form of ZnO and to a less extent in the form of $ZnO{\cdot}2ZnSO_4$, along with possibly a very small amount of remaining ZnS and willemite (Zn_2SiO_4). This means that the willemite formation started even before the completion of the second stage, as explained above. The ΔG of willemite formation at 700 °C is -29.5 kJ/mol which indicates that reaction in Eq. (15) is likely to occur (Bale and Bélisle, 2009). As there is no intermediate compound between $Y_2O_2S:Eu^{3+}$ and $Y_2(SO_4)_3:Eu^{3+}$, we concluded that the conversion of $Y_2O_2S:Eu^{3+}$ into $Y_2(SO_4)_3:Eu^{3+}$ proceeded via the reaction in Eq. (16), producing ZnO and SO_2 gas. It is unclear whether $Y_2O_2S:Eu^{3+}$ can also react with the intermediate $ZnO{\cdot}2ZnSO_4$, since it can be formed and consumed by the reactions between ZnS and $ZnSO_4$. However, it is clear that Eq. (16) is also dependent on the molar ratio of $ZnSO_4$:ZnS and their thermal interactions since it consumes $ZnSO_4$ as well.

$$2\ ZnO + SiO_2 \rightarrow Zn_2SiO_4 \quad (15)$$

$$Y_2O_2S + 6\ ZnSO_4 \rightarrow Y_2(SO_4)_3 + 6\ ZnO + 4\ SO_2 \quad (16)$$

When the calcine obtained by the ZSMH/CRT ratio of 3 and roasting at 700 °C for 2 h was leached in water, all the peaks of $Y_2(SO_4)_3:Eu^{3+}$ disappeared in the XRD pattern of the residue (Fig. 2(d)). This indicates that the majority of the REE sulfates dissolved. Although all other forms of Zn (ZnO, ZnS and Zn_2SiO_4) are poorly soluble in water, the intermediate complex $ZnO{\cdot}2ZnSO_4$ is partially soluble in water due to its sulfate content. That is the reason why all the

peaks related to this complex were replaced by that of a new phase, basic zinc sulfate or $ZnSO_4 \cdot 3Zn(OH)_2$. In aqueous environments, the concentration of possible Zn species largely depends on the pH of the solution. At pH < 6 (i.e. acidic solutions) $Zn^{2+}_{(aq)}$ is the main species, in neutral to slightly alkaline solutions, solid $Zn(OH)_2$ or ZnO are present and at pH = 12 or higher, $Zn(OH)_4^{2-}{}_{(aq)}$ is the dominant Zn species. Eqs. (17)-(21) summarize the pathways of their formation in aqueous solutions (Moezzi et al., 2011). Although $Zn(OH)^{+}_{(aq)}$ is the product of Eq. (17), it is replaced by a complex basic salt such as $ZnSO_4 \cdot 3Zn(OH)_2$ when the concentration of the hydroxide anion is not high enough to enable solid $Zn(OH)_2$ formation via Eq. (18). As this is observed in Fig. 2(d) where there is no $Zn(OH)_2$, the pH of the resulting leachate must be close to, but less than 7, indicating an insufficient amount of hydroxide ions. A pH measurement of that leachate proved it to be 6.1 ± 0.2. An external supply of OH^- via base addition could stimulate solid $Zn(OH)_2$ formation and increase the Zn removal from the leachate. However, the pH level is already close to the precipitation pH of REE hydroxides (i.e. 7-8.5) (Önal et al., 2015). Hence, without a close pH control, such a disturbance would most likely initiate the precipitation of REE hydroxides, resulting in significant REE losses to the residue.

$$Zn^{2+}_{(aq)} + OH^-_{(aq)} \rightarrow Zn(OH)^{+}_{(aq)} \quad (17)$$

$$Zn(OH)^{+}_{(aq)} + OH^-_{(aq)} \rightarrow Zn(OH)_{2(s)} \quad (18)$$

$$Zn(OH)_{2(s)} \leftrightarrows Zn(OH)_{2(aq)} \quad (19)$$

$$Zn(OH)_{2(aq)} + OH^-_{(aq)} \rightarrow Zn(OH)_3^-{}_{(aq)} \quad (20)$$

$$Zn(OH)_3^-{}_{(aq)} + OH^-_{(aq)} \rightarrow Zn(OH)_4^{2-}{}_{(aq)} \quad (21)$$

Based on the XRD results given in Figs. 1 and 2, the first quantitative experiments were performed with a ZSMH/CRT ratio of 3 for roasting duration of 1 or 3 h at varying roasting temperatures. As shown in Fig. 3, for both roasting durations, the percentage leaching of REEs increased from 75–80% at 600 °C to 96–98% at 700 °C while the percentage leaching of Zn drastically dropped from 50–55% to ca. 20% at 700 °C and even to as low as ca. 5% at 750 °C. Consistent with Fig. 1, the majority of Zn seemed to be in soluble form as an excess of dehydrated $ZnSO_4$ or $ZnO{\cdot}2ZnSO_4$ at low temperatures (i.e. < 700 °C). Meanwhile, a certain portion of REEs was still entrapped in the water-insoluble $Y_2O_2S{:}Eu^{3+}$ that did not react with $ZnSO_4$ yet. For that reason, roasting at temperatures of 600 and 650 °C was abandoned in the rest of the study due to slow reaction kinetics, even after 3 h with a ZSMH/CRT ratio of 3. Although ≥ 95% of REEs was extracted at 700 and 750 °C for both durations (1 and 3 h), the purity of the leachates was not sufficiently high due to remaining $ZnO{\cdot}2ZnSO_4$. The resulting concentration ratios ([REE]/[Zn]) were ca. 0.65 and 2.10, respectively, compared to 0.54 wt./wt.% [REE]/[Zn] in the initial CRT powder. Hence, some selectivity for the REEs over Zn was already achieved, but further minimization of the Zn co-dissolution, ideally to < 1%, is preferred. At the same time, the leaching efficiency of the REEs should be preserved at > 90%, so the selectivity can be improved. Co-dissolution of Zn should be avoided as much as possible to produce a pure REE leachate suitable for subsequent purification with solvent extraction to separate Y and Eu. The following experiments aimed at further optimizing the selectivity for the REEs over Zn.

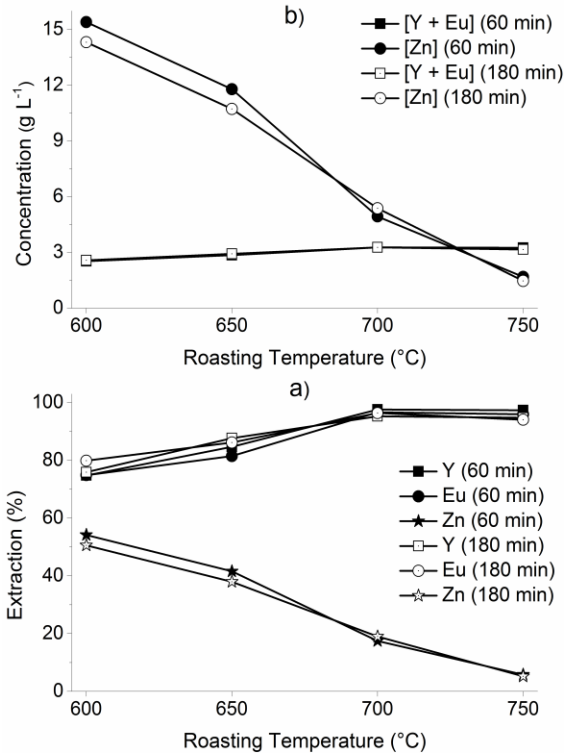

Fig. 3. Effect of roasting temperature and duration on a) percentage metal leaching and b) metal concentrations (fixed conditions: ZSMH/CRT ratio of 3, 20 g L^{-1} CRT concentration, 24 h of water leaching at 25 °C).

3.3. Effect of Amount of Added Zinc Sulfate Monohydrate

The first parameter that was optimized was the added amount of zinc sulfate monohydrate (ZSMH). This amount must be high enough to complete the conversion of ZnS to ZnO and $Y_2O_2S:Eu^{3+}$ to REE sulfates, but an excess would lead to the undesirable formation of the water-soluble intermediate $ZnO{\cdot}2ZnSO_4$ complex. In Fig. 4(a), the percentage leaching of REEs at 700 °C gradually declined towards 85–90% with a decrease of the amount of added ZSMH. This decrease was more drastic (to 50%) in the case of roasting at 750 °C (Fig. 4(b)). On the other hand, the percentage leaching for Zn showed a more drastic decrease at 700 °C, from ca. 20% to

ca. 6% when the added amount of ZSMH was decreased. At 750 °C, only a slight change was visible in its already low percentage leaching (ca. 3-6%).

In general, when less ZSMH is present in the roasting mixture, more $Y_2O_2S:Eu^{3+}$ and ZnS are potentially exposed to air oxidation. In the absence of ZSMH, both ZnS and $Y_2O_2S:Eu^{3+}$ are oxidized more by air at higher temperatures (Figs. 1 and 2). In the case of the REEs, this results in the formation of the more poorly soluble intermediate oxide sulfates, $Y_2O_2SO_4:Eu^{3+}$ or $2Y_2O_3{\cdot}Y_2(SO_4)_3:Eu^{3+}$, instead of the comparatively very soluble $Y_2(SO_4)_3:Eu^{3+}$. Hence, there is a certain competition between ZSMH and air to react with $Y_2O_2S:Eu^{3+}$. Fig. 4(a) shows that the same amounts of ZSMH still allows high leaching percentages for REE at 700 °C, indicating that this cannot be the sole reason for the drastic decrease at 750 °C. Based on the reactions in Eqs. (14) and (16), the conversion of both $Y_2O_2S:Eu^{3+}$ and ZnS consumes ZSMH, which in turn results in a natural competition between them for the available $ZnSO_4$. However, at temperatures above 700 °C, the thermal decomposition of $ZnSO_4$ to $ZnO{\cdot}2ZnSO_4$ also intensifies, consuming additional $ZnSO_4$ before it can react with $Y_2O_2S:Eu^{3+}$. The reason why increasing the ZSMH/CRT ratio to 3 restored the percentage leaching for REEs to almost 100% is simply due to compensation for this additional mechanism and simultaneously decreasing the probability of air oxidation of $Y_2O_2S:Eu^{3+}$. Similarly, the leaching of the REEs is affected less at 700 °C as there is less thermal decomposition of ZSMH and thus less need for ZSMH compensation. This reasoning also implies that $ZnO{\cdot}2ZnSO_4$ is less or even not able to convert $Y_2O_2S:Eu^{3+}$ to REE sulfates and the conversion can only occur in the presence of free $ZnSO_4$.

Once again, the effect of roasting duration under these conditions was found to be negligible, possibly due to an equilibrium between the phases at these two roasting temperatures. Hence, longer roasting durations and/or higher temperatures are required to disturb this equilibrium in

favor of complete decomposition of the remaining $ZnO{\cdot}2ZnSO_4$ to ZnO. A roasting time of 3 h was already long enough and longer roasting times were considered impractical and thus not studied.

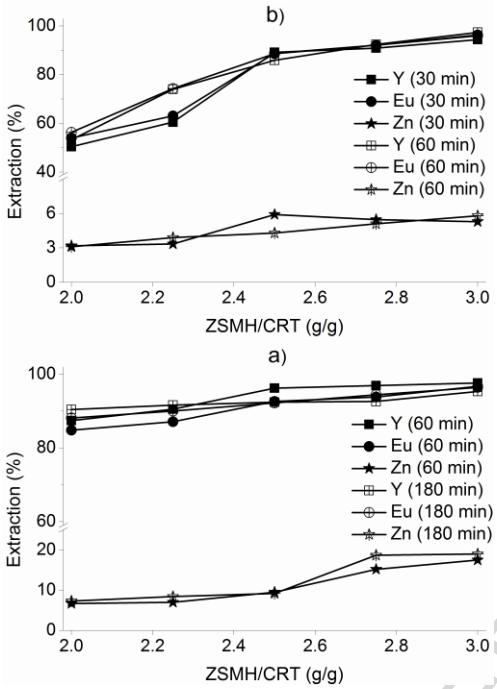

Fig. 4. Effect of the $ZnSO_4{\cdot}H_2O$ (ZSMH) to CRT ratio on the Y, Eu and Zn extraction (%) when roasted at a) 700 °C for 1 or 3 h and b) 750 °C for 0.5 or 1 h (fixed conditions: 20 g L^{-1} CRT concentration, 24 h of water leaching at 25 °C).

3.4. Effect of Roasting Temperature and Duration

Although a ZSMH/CRT ratio of 3 ensures the full conversion of $Y_2O_2S{:}Eu^{3+}$ and ≥ 95% REE leaching, it also results in a certain amount of remaining $ZnO{\cdot}2ZnSO_4$ and persistent 5% co-dissolution of Zn even after 3 h of roasting. To solve this issue, roasting temperatures higher than 750 °C with a ZSMH/CRT ratio of 3 were tested to investigate the possibility of decomposing

the remaining intermediate complex to ZnO without decomposition of the water-soluble REE sulfates.

In Fig. 5, only at a temperature of 900 °C and after 1 h of roasting it was possible to reduce the percentage leaching of Zn to less than 1%. All other tested conditions resulted in higher percentage leaching of Zn. Hence, the thermal decomposition of the intermediate complex was completed at much higher temperatures than expected from literature (Malinowski and Malinowska, 1994). This could be due to the differences in the experimental conditions, as explained in Section 3.2. Unfortunately, the percentage leaching of REEs started to drop below 90% already at 800 °C after 45 minutes of roasting and to even much lower levels at higher temperatures in much shorter roasting durations. As explained above, this is due to faster thermal decomposition of free $ZnSO_4$ before it could react with $Y_2O_2S{:}Eu^{3+}$ and form REE sulfates. Moreover, the newly formed REE sulfates also start to decompose at temperatures above 800 °C to give the corresponding oxysulfates, $REE_2O_2SO_4$, and SO_2 gas. The very poor solubility of the REE oxysulfates in water could explain the significant reduction in their percentage leaching (Önal et al., 2015). Based on these results, it can be concluded that the selectivity for REEs over Zn could not be improved significantly without reducing the leaching of REEs by only modifying the roasting conditions. To summarize, the reasons for this behavior are: (i) the thermal decomposition temperature of the remaining partially soluble $ZnO{\cdot}2ZnSO_4$ is quite close to that of the REE sulfates, (ii) $ZnO{\cdot}2ZnSO_4$ is not as effective as the free $ZnSO_4$ to convert $Y_2O_2S{:}Eu^{3+}$ to REE sulfates and (iii) the competition between ZnS, $Y_2O_2S{:}Eu^{3+}$ and the thermal decomposition of $ZnSO_4$ to give $ZnO{\cdot}2ZnSO_4$ complicates the optimization process. Therefore, further tests focused on the water leaching parameters for which the following optimal roasting conditions were selected: ZSMH/CRT ratio of 3, a roasting temperature of 750 °C and 30 min of

roasting time, yielding 94.7% Y, 96.3% Eu and 5.29% Zn leaching after water leaching with the CRT concentration of 20 g L^{-1} at 25 °C for 24 h.

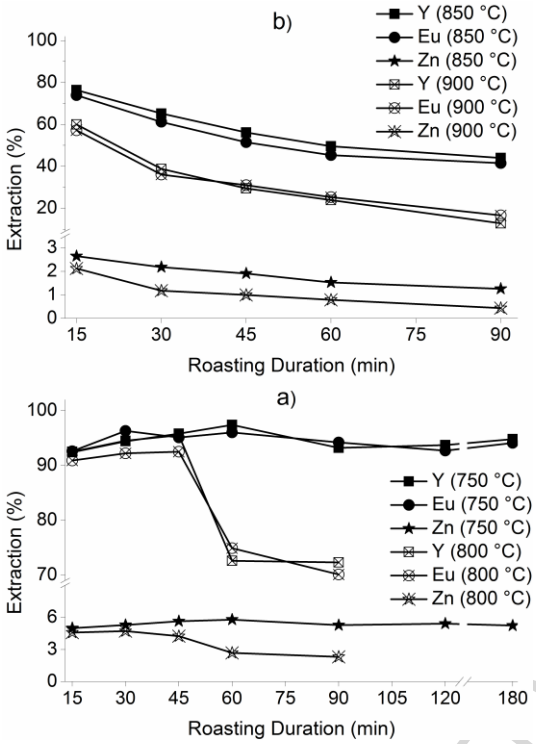

Fig. 5. Effect of roasting temperature and duration on Y, Eu and Zn leaching (%) at a) 750 and 800 °C and b) 850 and 900 °C (fixed conditions: ZSMH/CRT ratio of 3, 20 g L^{-1} CRT concentration, 24 h water leaching at 25 °C).

3.5. Effect of Water Leaching Parameters

In Table 2, the percentage leaching of the metals and the resulting metal concentrations and their ratios are given for three different CRT concentrations after varying the water leaching durations. Considering the already low solubility of REE sulfates in water (e.g. 1.8 g/100 g of H_2O for $Eu_2(SO_4)_3 \cdot 8\ H_2O$ at 40 °C) and the fact that their solubility tends to decrease with increasing temperatures, the leaching temperature was not considered as a parameter (Önal et al., 2015).

In general, for all CRT concentrations, the dissolution rate of the REE sulfates are quite fast, giving 90-96% leaching after only 1 h of leaching. With a decrease in quantity of water (i.e. increasing CRT concentration), there was a slight decrease to 90% due to less available solvent. However, the percentage leaching tends to decrease more noticeably after a certain period of water leaching. This threshold duration seems to depend on the CRT concentration and extends to longer durations for higher water content. For example, the REE percentage leaching remained around 95% for 20 g L^{-1} even after 48 h of leaching, but then decreased to 90% after 96 h of leaching. Meanwhile, for a CRT concentration of 100 g L^{-1}, the leaching efficiencies of the REEs decreased more drastically to < 80% only after 48 h of leaching. A similar change can be expected for a CRT concentration of 40 g L^{-1} between 24 and 48 h. This threshold duration could result from an aging effect which was visually observed in the stored leachates after 24 h of leaching. While twice-filtered and analyzed samples from 20 g L^{-1} CRT concentration experiments remained transparent for weeks, those obtained from 40 or 100 g L^{-1} CRT concentration experiments became turbid after about one week or a couple of days, respectively. Re-analysis of these leachates after filtration showed a decrease in the percentage leaching of REEs compared to the original values. However, the visual aging of the samples disappeared from then on indicating that an equilibrium was reached in the samples. The reason why the aging requires shorter durations during water leaching than in the filtered solutions can be attributed to the differences in the nucleation type of the precipitates. The solid particles that do not dissolve during water leaching can act as heterogeneous nucleation sites or "seeds", thereby accelerating the aging process compared to more time-consuming homogenous nucleation observed in the filtered solutions.

Table 2 Effect of leaching parameters on percentage extraction of metal, concentration and concentration ratio.

CRT Concentration (g L^{-1})	20					40			100				
Leaching Duration (h)	1	6	24	48	96	1	6	24	1	6	24	48	96
Metal	Extraction (%)												
Y	93.8	94.6	94.7	95.0	91.4	93.2	93.6	93.5	92.5	92.3	91.5	79.3	71.8
Eu	95.8	96.1	96.3	95.5	91.5	94.0	95.5	94.9	93.7	92.5	91.5	70.6	62.1
Zn	14.5	9.10	5.29	4.40	4.32	12.8	8.40	4.80	9.60	6.50	2.70	2.10	2.00
Metal	Concentration (ppm)												
[Y+Eu]	3152	3192	3183	3175	3059	6220	6281	6275	15537	15385	15673	13146	11874
[Zn]	4097	2570	1490	1233	1220	7253	4713	2718	13562	9164	3834	2955	2801
[Y+Eu]/[Zn]	0.77	1.24	2.14	2.57	2.51	0.86	1.33	2.31	1.15	1.68	4.09	4.45	4.24

Fixed conditions: ZSMH/CRT ratio of 3, 750 °C and 30 min roasting.

The trend observed for REEs percentage leaching in Table 2 is also valid for the behavior of Zn. With longer leaching durations or higher CRT concentrations, the Zn percentage leaching decreases similarly as in the case of the REEs. However, after the so-called threshold time, the effect of leaching time becomes negligible. This means that the soluble portion of the intermediate $ZnO{\cdot}2ZnSO_4$ quickly dissolves at the very early stage of the leaching, similarly to the REE sulfates. In the remaining leaching period, the dissolved Zn ions slowly hydrolyze via Eq. (17), forming the basic zinc sulfate $ZnSO_4{\cdot}3Zn(OH)_2$. This results in the continuous decrease of the percentage leaching of Zn until a certain amount of Zn ions can reach an equilibrium and remain in the leachate. Hence, it is anticipated that the sluggish hydrolysis of Zn ions could be the cause of aging that also negatively affects the percentage leaching of REEs over time. As

stated in Section 3.2, during the water leaching stage the only possible mechanism that could cause REE losses is the precipitation of REE hydroxides. Therefore, while Zn is reaching an equilibrium through hydrolysis, it must also alter the chemistry of the leachate (e.g. pH) in favor of REE hydroxide formation. This effect becomes more prominent when the Zn (and thus REEs) concentration is higher in the leachate.

3.5.1. Effect of ethylene glycol (EG) amount

Although the REE percentage leaching is comparatively lower, the highest selectivity values were obtained for the lowest amount of water (i.e. 100 g L^{-1}) for all studied leaching durations. Hence, it could be possible to reduce the Zn co-dissolution below 1% by increasing the CRT concentration above 100 g L^{-1}, but at the expense of REE losses to the residue. It is also worth mentioning that the sludge obtained after 100 g L^{-1} CRT experiments was already highly dense due to high quantities of solid and low quantities of water. This could become problematic for efficient solid-liquid (S/L) separation at larger scales.

Alternatively, leaching with an organic solvent was examined to reduce the amount of water. Ethylene glycol (EG) was tested because of its ability to dissolve REE sulfates. As shown in Fig. 6(a), the same high REE percentage leaching could be obtained when up to 80 vol.% of water was replaced by EG, for both 20 and 40 g L^{-1} CRT concentrations. That is because EG has a polarity index of 0.79, which is close to that of water (polarity index of 1.00) (Murov, 2010). However, complete water replacement by EG causes a noticeable decrease in the REE leaching to 80% indicating that the solubility of REE sulfates is lower in pure EG than in pure water. On the other hand, the percentage leaching of Zn remained at the same low level of about 5% until 50 vol.% replacement of water by EG and then gradually increased in higher EG concentrations.

Most likely, EG is able to dissolve the intermediate $ZnO{\cdot}2ZnSO_4$. Furthermore, the subsequent hydrolysis of Zn via Eq. (17) probably decreases if less water is present, which means that the formation of solid $ZnSO_4{\cdot}3Zn(OH)_2$ is hindered or even prevented, resulting in a higher percentage leaching of Zn. Based on the percentage leaching of Zn in pure EG (~20% Zn leaching) and in pure water (~5% Zn leaching), the hydrolysis mechanism during water leaching accounts for a decrease in Zn leaching of ~15%. In other words, ~20% of the Zn content in the calcine is soluble and present in the form of $ZnO{\cdot}2ZnSO_4$, which is the only possible soluble Zn source. The remaining ~80% of Zn must be in the form of water-insoluble ZnO, ZnS or Zn_2SiO_4. Therefore, it can be stated that a certain equilibrium is established between the phases of the residue and the species of the leachate during the water leaching step. As a result of this equilibrium, it is not possible to reduce the leaching of Zn below 1% without also compromising the REE leaching, so contamination of the REE-rich leachate with Zn is unavoidable when maintaining an acceptably high REE percentage leaching (i.e. > 90%). Since replacing water with EG did not improve the selectivity, this part of the work was not studied further.

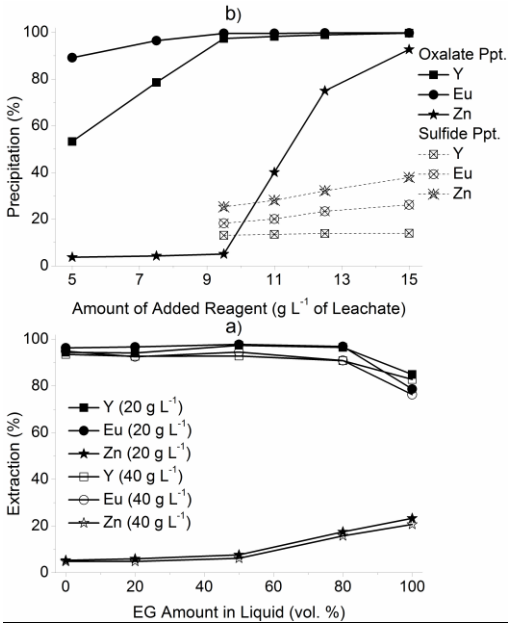

Fig. 6. a) Effect of the amount of ethylene glycol (EG) in the total liquid volume on the percentage leaching of metal (fixed conditions: ZSMH/CRT ratio of 3, 750 °C and 30 min roasting) and b) effect of the added reagent amount on the percentage precipitation of metal for the oxalate and sulfide precipitation methods (fixed conditions: 700 rpm, 1 h at 25 °C).

3.5.2. Optimum conditions and sample characterization

A stock leach solution was generated using the optimum roasting and water leaching conditions, giving 93.5%, 94.9% and 4.80% leaching efficiencies for Y, Eu and Zn, respectively. The composition of the leach solution is given in Table 3 along with the optimum conditions. In Fig. 7, the XRD patterns of the obtained calcine (CRT powder after roasting) and the residue after leaching under optimum conditions are compared with the preliminary tests, also shown in Fig. 2 (c) and (d). The patterns for both the calcine and the residue are comparable with the preliminary results, meaning that the differences in metal leaching are mostly due to the differences in the phase quantities. The chemical composition of the leach residue obtained under these optimum conditions is given in Table 3. As a result of the addition of ZSMH, the low leaching of Zn and

the high leaching of the REE, the residue is highly enriched in Zn. Since sulfur is mostly associated with the basic zinc sulfate, it is the second major element followed by minor impurities such as Al, Pb and Si, which were also present in the initial CRT waste powder (Table 1). This indicates that the impurities report to the leaching residue and that the sulfation reactions are highly selective towards ZnS and $Y_2O_2S:Eu^{3+}$ only. Thus, the produced leachate should already be highly pure in REEs except for a certain contamination of Zn.

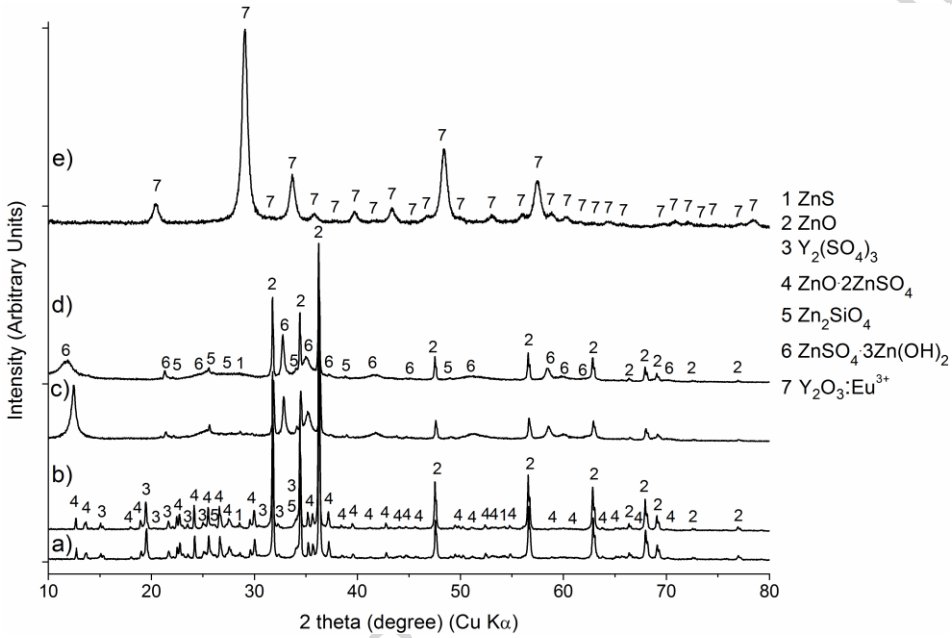

Fig. 7. XRD patterns of the a, b) calcines and c, d) the residues obtained with the preliminary tests and the optimum conditions, respectively, along with e) the mixed REE oxide obtained after calcination at 750 °C for 6 h.

Table 3 Chemical composition of the stock solution and the leach residue obtained under optimum conditions.

Sample	Metal Concentration (ppm) (Leaching efficiency)									
Leachate	Y		Eu		Zn		[REE]/[Zn]			
	5900 ± 100 (93.4%)		362 ± 50 (94.9%)		2650 ± 100 (4.80%)		2.35 ± 0.15			
	Metal Oxide (wt.%)									
Leach Residue	Y_2O_3	Eu_2O_3	ZnO	SO_3	CaO	CdO	PbO	K_2O	SiO_2	Al_2O_3
	0.31	0.04	77.7	13.8	0.08	0.03	1.31	0.11	2.45	2.07
	SrO	BaO	ZrO_2	Fe_2O_3	CoO	TiO_2	CuO	Cr_2O_3	NiO	Total
	0.97	0.71	0.18	0.10	0.05	0.04	0.03	0.01	0.01	100.0

Fixed conditions: ZSMH/CRT ratio of 3, 30 min roasting at 750 °C, 24 h water leaching at 25 °C with 40 g L^{-1} CRT concentration.

3.6. Purification Methods

Since it was not possible to obtain a pure REE leachate at the optimum roasting and leaching conditions, without partial co-dissolution of Zn, the leachate was further purified by selective precipitation. First, sulfide precipitation was tested but the preliminary tests gave no selectivity against Zn, not even with the smallest amount of added reagent (Fig. 6(b)). This is primarily caused by close-to-neutral pH of the leachate (e.g. pH 6.1) that could promote the co-precipitation of REEs as sulfides and/or hydroxides which was also observed in the literature (Innocenzi et al., 2013a). Hence, without addition of an acid to reduce the pH level, the sulfide precipitation option cannot offer an effective solution for selective separation of REEs from Zn. Despite the high pH of the leachate, high selectivity is still expected for oxalate precipitation due to the much lower solubility of REE oxalates compared to those of the transition metal oxalates.

More specifically, the K_{sp} of ZnC_2O_4 is equal to 1.5×10^{-9}, while the K_{sp} of $Y_2(C_2O_4)_3$ is only 5.1×10^{-30} (Chung et al., 1998; Da Silva et al., 2010). In Fig. 6(b), direct addition of solid oxalic acid in a stoichiometric amount, namely 9.5 g L^{-1}, resulted in almost complete precipitation of the REEs with 5% co-precipitation of Zn. The oxalate precipitation reactions for the REEs and Zn are described by Eqs. (22)-(23). Since acid is released during the oxalate precipitation, low pH and/or the presence of an excess of H_2SO_4 hinders the formation of the oxalates and an excess of oxalic acid will be required for quantitative precipitation (Chung et al., 1998). Considering that the solubility of Zn oxalate is much higher than the REE oxalates, the co-precipitation of Zn can be optionally lowered to less than 5% by adding small aliquots of H_2SO_4.

$$REE_2(SO_4)_{3(aq)} + 3\ H_2C_2O_{4(s)} \leftrightarrow REE_2(C_2O_4)_{3(s)} + 3\ H_2SO_{4(aq)} \quad (22)$$

$$ZnSO_{4(aq)} + H_2C_2O_{4(s)} \leftrightarrow ZnC_2O_{4(s)} + H_2SO_{4(aq)} \quad (23)$$

The oxalate precipitate obtained by addition of 9.5 g L^{-1} of oxalic acid was calcined at 750 °C. After 6 h of calcination, the associated mass loss stabilized at 53.6%. The composition of the mixed REE oxide measured by both semi-quantitative WD-XRF and ICP-OES is given in Table 4. Despite the difference for the Y_2O_3 and Eu_2O_3 content between the two techniques, a total of 97.4 wt.% was formed by REE oxides with only 2.2 wt.% of ZnO. Only few other impurities with negligible quantities were detected by WD-XRF. This indicates that the leachate after water leaching was already highly pure containing almost only REEs and Zn while the rest of the impurities were left in the zinc-rich solid residue (Table 3). In agreement with its composition, the XRD pattern of the mixed REE oxide in Fig. 7(e) shows only crystalline Y_2O_3:Eu^{3+} peaks

due to the low ZnO content. It is also comparable with the XRD pattern of the mixed REE oxide obtained in reference (Yin et al., 2016).

Table 4 Chemical composition of the mixed REE oxide obtained under optimum conditions based on ICP-OES and WD-XRF methods.

Sample	Method	Compound (wt.%)									
		Y_2O_3	Eu_2O_3	ZnO	SO_3	CaO	CdO	PbO	K_2O	Others	Total
Mixed Oxide	ICP-OES	92.0	5.42	2.23	NA	NA	NA	NA	NA	0.35	100.0
	WD-XRF	89.0	7.97	2.40	0.43	0.06	0.06	0.03	0.02	-	100.0

ZnO is the only impurity present in significant amounts and can be washed away from the mixed REE oxide by a diluted alkaline solution, based on its amphoteric properties. Since the REE oxides are not soluble in alkaline conditions, the small amount of ZnO can be selectively removed from the mixed REE oxide without causing any REE oxide losses. In principle, the alkaline solution could be reused for several cycles, accumulating the dissolved Zn. After a certain accumulation, the dissolved Zn can be recovered by hydrometallurgical methods, such as electro-winning, to produce metallic Zn while the depleted wash solution can be recirculated to the flow sheet, similarly as described in the literature (Zhang et al., 2014). Meanwhile, the remaining high quantity of Zn in the leaching residue can be recovered by contact with the leachate after oxalate precipitation. According to Eqs. (22)-(23), three moles of H_2SO_4 are generated in the leachate for the precipitation of one mole of REE sulfate with oxalic acid, which might be sufficient to dissolve all Zn in the leaching residue. In case additional H_2SO_4 is needed for complete dissolution of Zn, the flue gas (SO_2) of the roasting step can be collected and forwarded to an acid plant for generation of sulfuric acid for that purpose. This way, it is possible

to recover almost all of the Zn in the flow sheet by conventional hydrometallurgical methods (Fig. 8).

Based on these results, hydroxide precipitation can also be tested as an alternative to the oxalate precipitation. The pH of the leachate after water leaching is already close to neutral (e.g. 6.1). By introducing small aliquots of a base solution (e.g. NaOH), all of the REEs and Zn can be precipitated as their respective hydroxides at pH 7.5-8. However, by further increasing the pH, the zinc hydroxide can be selectively re-dissolved via Eqs. (20)-(21) leaving the REE hydroxides in the solid precipitate. After a similar calcination treatment in Fig. 8, a mixed REE oxide with higher purity (> 97.4 wt.%) can be directly obtained without an alkaline washing step for ZnO removal. This way, the flue gas of the calcination treatment (CO_2) can be replaced by a greener option (H_2O) too. The REE-depleted but Zn-containing basic leachate can then be forwarded to the leaching of the amphoteric ZnO and $ZnSO_4{\cdot}3Zn(OH)_2$ in the leach residue allowing a potentially complete Zn recovery. However, gelatinous nature of the hydroxide precipitates will require a more efficient S/L separation compared to the case of highly crystalline oxalates. Otherwise, a certain contamination of the mixed REE oxide by especially the base (e.g. NaOH) will be unavoidable.

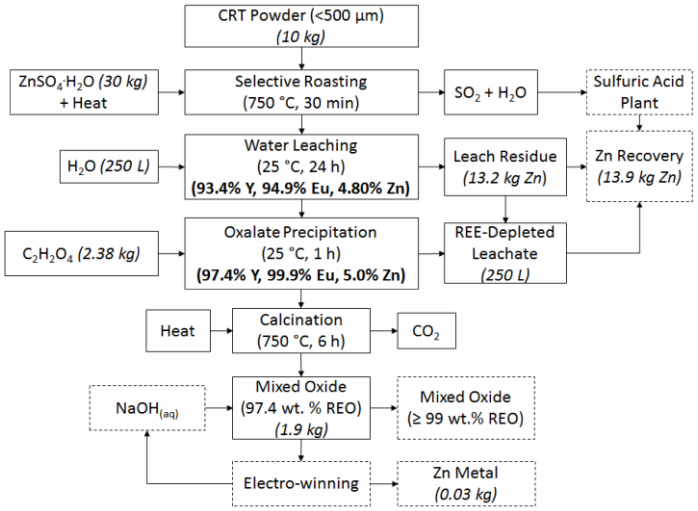

Fig. 8. Proposed overall flow sheet based on oxalic acid purification (purification route 1). Mass balance and leaching or precipitation % of metals are given for the proposed optimum conditions. The dashed lines have not been studied experimentally in this work.

As an alternative to oxalate precipitation, a new method was tested, inspired by works on zinc ash or fly dust from smelting operations (Thorsen et al., 1984; Thorsen and Grislingas, 1981). In these studies, it was shown that an acidic leachate containing Zn(II) sulfate can be purified from co-dissolved iron(III) sulfate by a solvometallurgical method. For that purpose, 30 vol.% Versatic acid (VA) in an aliphatic diluent (i.e. *n*-dodecane) was first loaded with Zn(II), by reaction with ZnO. Next, the Zn(II)-loaded VA phase (organic phase) was then contacted with the Fe(III)-containing Zn(II)-leachate (aqueous phase), forming a biphasic mixture. Consequently, the Fe(III) from the aqueous phase exchanged with the Zn(II) from the organic phase by liquid-liquid exchange reaction, due to the higher affinity of Fe(III) for the VA in the organic phase. In this way, all Fe(III) was removed from the aqueous phase, leaving behind a pure zinc-containing aqueous solution. Since the leach residue in our study contains significant

quantities of ZnO (Fig. 7) and the leachate contains a certain concentration of Zn, a similar concept was tested where REE(III) ions from the leachate (aqueous phase) are exchanged with Zn(II) ions from Zn(II)-VA (organic phase) (Eq. 24). It is important to have a full exchange, so that the organic phase is completely depleted in Zn and pure in REEs. Based on Eq. 24, the stoichiometric concentration of Zn(II) in the organic phase is calculated to be 6.5 g L^{-1} for a 1:1 organic-to-aqueous (O/A) volume ratio, assuming that the reaction goes to completion.

$$REE_2(SO_4)_{3(aq)} + 3\ Zn(VA)_{2(org)} \leftrightarrow 2\ REE(VA)_{3(org)} + 3\ ZnSO_{4(aq)} \quad (24)$$

However, the experimental results showed that the percentage extraction of Y and Eu remained around 77% and 87%, respectively, in exchange for ~77% of the initial Zn(II) in the organic phase (Table 5). These results could not be improved by varying the O:A volume ratio by addition of free VA to the Zn(II)-loaded organic phase or by increasing the contact time to 24 h. This means that more than a stoichiometric concentration of Zn(II) is required to push the equilibrium in Eq. (24) to completion.

Table 5 Effect of organic-to-aqueous phase (O:A) ratio on metal extractions with different initial zinc concentrations in the concentrated Versatic acid (VA).

O:A ratio (vol:vol%)	Y extraction to VA (%)	Eu extraction to VA (%)	Zn extraction to leachate (%)	Initial Zn in VA (ppm)	Final Zn in VA (ppm)	Final [REE]/[Zn] in VA (ppm/ppm)
10	76.9	86.9	77.4	650 ± 10	123	3.25 ± 0.50
5	78.8	87.7	78.3	1300 ± 100	352	
2.5	77.1	86.3	77.5	2600 ± 100	594	
1	75.5	83.5	79.6	6500 ± 100	1306	

Fixed conditions: 2000 rpm, 1 h, 30 °C.

When the influence of the O:A ratio was studied by varying the volume of VA loaded with 6.5 g L^{-1} Zn(II), instead of diluting with pure VA, the situation changed (Table 6). In this way, a higher amount of Zn(II) than stoichiometrically required was introduced into the biphasic mixture. This resulted in an almost complete extraction of REEs to the organic phase in exchange for a small portion of the initial amount of Zn(II) in the organic phase. With O:A ratios smaller than 1, almost all Zn(II) in the organic phase transferred to the aqueous phase, in exchange for a small portion of the REEs. Based on these observations, the best option here would be to use a small O:A ratio (i.e. 0.10), so an organic phase pure in REEs is obtained, and performing the purification in more than one step. After each contact, a portion of the REEs can be extracted to Zn(II)-loaded organic phase which becomes completely depleted in Zn(II).

Table 6 Effect of organic-to-aqueous phase ratio (O:A) on metal extractions with the same initial zinc concentration (6500 ± 100 ppm) in the concentrated Versatic acid (VA).

O:A ratio (vol:vol%)	Y extraction to VA (%)	Eu extraction to VA (%)	Zn extraction to leachate (%)	Final Zn in VA (ppm)	Final [REE]/[Zn] in VA (ppm/ppm)
10	99.9	99.7	11.3	5690	0.11
5	99.9	99.7	20.6	5091	0.24
1	75.5	83.5	79.6	1306	3.56
0.50	43.4	56.7	89.1	700	7.74
0.25	23.9	35.2	90.7	597	10.1
0.10	11.0	16.5	96.8	208	33.3

Fixed conditions: 2000 rpm, 1 h, 30 °C.

Next, the extracted REEs can be stripped from the organic phase by H_2SO_4 to a highly pure aqueous solution, which can be directly applied to solvent extraction to separate the different REEs. The regenerated VA can be re-loaded with Zn(II) and recirculated into the flow sheet, with minimal losses due to the low solubility in the aqueous phase. Once the leachate is depleted

in REEs, it can be treated further for the recovery of the accumulated Zn along with the remaining Zn in the leaching residue. However, further studies are needed to experimentally test these ideas. An overview of this second purification route is depicted in Fig. 9.

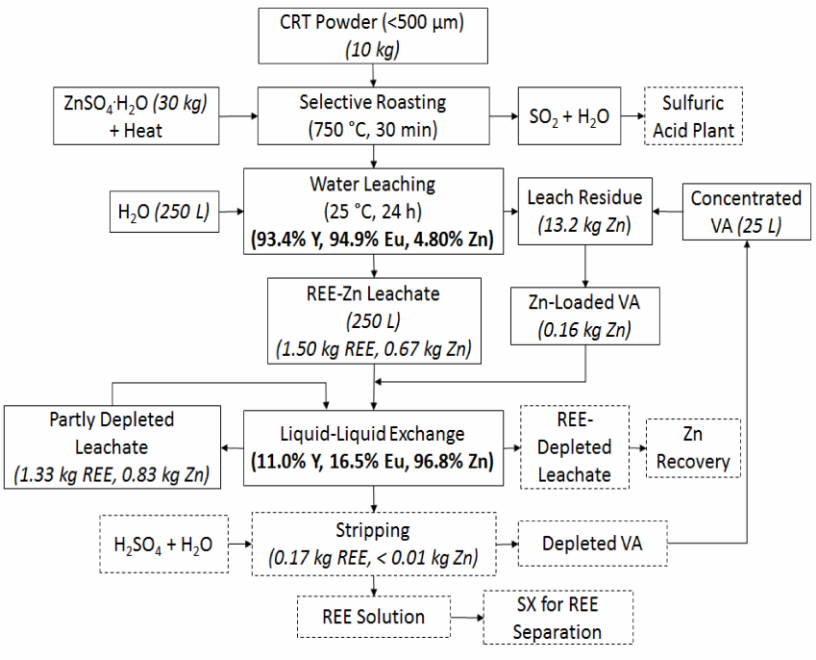

Fig. 9. Proposed overall flow sheet based on Versatic acid purification (purification route 2). Mass balance and leaching or extraction % of metals are given for the proposed optimum conditions. The dashed lines have not been studied experimentally in this work.

Between the two proposed flow sheets, the first purification route (Fig. 8) is considered more desirable. Although only the consumed oxalic acid is not recyclable, a very high-purity mixed REE oxide can be obtained through a more conventional and straightforward process compared to the VA case (Fig. 9). This flow sheet can be further improved by testing the hydroxide precipitation by a base solution instead of oxalate precipitation. On the other hand, if the individual REE oxides have to be obtained as the final products, then the mixed REE oxide needs to be re-dissolved in an acidic solution for solvent extraction. This is not required in Fig. 9

since a REE-rich leachate can be directly produced for solvent extraction while regenerating the consumed VA for re-use in the flow sheet.

Conclusions

In this study a new flow sheet was developed for the selective recovery of rare earths from CRT phosphor waste powder avoiding direct attack by strong acids or bases. In this flow sheet the formation of toxic H_2S gas, the need for adding an oxidizing agent and the release of unwanted impurities present in the CRT powder are avoided. By addition of solid $ZnSO_4 \cdot H_2O$ and roasting the mixture at 700–750 °C, $Y_2O_2S:Eu^{3+}$ was selectively converted into the corresponding water-soluble rare-earth sulfates, while ZnS was largely transformed into water-insoluble ZnO and, to a lesser extent, into a partially water-soluble intermediate complex $ZnO \cdot 2ZnSO_4$. Formation of the difficult to dissolve willemite (Zn_2SiO_4) was greatly suppressed, so that Zn could be more easily recovered after removing the rare earths. The REEs were selectively extracted from the roasted CRT powder by leaching with water. More than 95% of the REEs were dissolved, leaving the majority of the Zn in the leaching residue. To decrease the persistent ca. 5% co-dissolution of total zinc, water was partially or completely replaced by ethylene glycol (EG). However, this resulted in a decrease in the leaching efficiencies of REEs to ca. 80% and a gradual increase in that of Zn to ca. 20%.

To further purify the obtained leachate and obtain a pure REE fraction without Zn impurities, three purification routes were tested. Sulfide precipitation gave no selectivity against Zn and not studied further. The second route involved oxalate precipitation giving > 97% REE precipitation but also ca. 5% Zn co-precipitation. The respective mixed oxide was made of 97. 4 wt.% REE oxides and 2.2 wt.% ZnO. . The third route involved a novel liquid-liquid extraction route for the

REEs with zinc(II)-loaded Versatic Acid. The REE-Zn exchange could not be completed in single contact when the Versatic Acid was loaded with stoichiometric amount of zinc. However, an excess amount of REEs in the leachate depleted the Zn content in the Versatic Acid (i.e. low O:A ratios). As in Fig. 9, 0.17 kg of 1.33 kg of REEs can be extracted in one contact to a highly pure organic solution with only 0.005 kg of zinc contamination. However, several contact cycles will be required to fully deplete the REEs from the leachate thereby complicating the flow sheet. Further studies (e.g. varying the pH of the leachate or addition of different sulfate salts before the exchange) could be tested to explore more this new approach.

In this study, the oxalate precipitation was selected as the preferred purification route because it is more conventional and straightforward. As in Fig. 8, a total of 1.90 kg of mixed rare-earth oxide with 0.03 kg of zinc contamination can be obtained by processing 10 kg of a CRT powder. Two possible methods were proposed to further improve this route and reduce the ZnO contamination in the final mixed oxide: washing off the ZnO by an alkali solution or replacing the oxalate precipitation by hydroxide precipitation at high pH levels (> 8). However, these methods have to be studied experimentally as a future work.

Acknowledgements

The authors thank the KU Leuven for financial support (projects GOA/13/008 and C32/17/011). The authors would like to thank Bieke Onghena for her help in revising the manuscript, Pieter L'hoëst for performing WD-XRF measurements and Federica Forte for helpful discussions.

References

Bale, C.W., Bélisle, E., 2009. Fact-Web suite of interactive programs [WWW Document]. URL http://www.crct.polymtl.ca/factweb.php (accessed 10.30.17).

Binnemans, K., Jones, P.T., Blanpain, B., Van Gerven, T., Yang, Y., Walton, A., Buchert, M., 2013. Recycling of rare earths: A critical review. J. Clean. Prod. 51, 1–22. doi:10.1016/j.jclepro.2012.12.037

Chung, D.-Y., Kim, E.-H., Lee, E.-H., Yoo, J.-H., 1998. Solubility of rare earth oxalate in oxalic and nitric acid media. J. Ind. Eng. Chem. 4, 277–284.

Ciftci, M., Cicek, B., 2017. E-waste: A review of CRT (cathode ray tube) recycling. Res. Rev. J. Mater. Sci. 05, 1–17. doi:10.4172/2321-6212.1000170

Da Silva, R.G., Da Silva, C.N., Afonso, J.C., 2010. Recovery of manganese and zinc from spent Zn-C and alkaline batteries in acidic medium. Quim. Nova 33, 1957–1961. doi:S0100-40422010000900024

De Michelis, I., Ferella, F., Varelli, E.F., Vegliò, F., 2011. Treatment of exhaust fluorescent lamps to recover yttrium : Experimental and process analyses. Waste Manag. 31, 2559–2568. doi:10.1016/j.wasman.2011.07.004

Dexpert-Ghys, J., Regnier, S., Canac, S., Beaudette, T., Guillot, P., Caillier, B., Mauricot, R., Navarro, J., Sekhri, S., 2009. Re-processing CRT phosphors for mercury-free applications. J. Lumin. 129, 1968–1972. doi:10.1016/j.jlumin.2009.04.080

Grause, G., Takahashi, K., Yoshioka, T., 2016. Thermogravimetric investigation of the lead volatilization from waste cathode-ray tube glass. Recycling 1, 111–121. doi:10.3390/recycling1010111

Herat, S., 2008. Recycling of cathode ray tubes (CRTs) in electronic waste. CLEAN – Soil, Air,

Water 36, 19–24. doi:10.1002/clen.200700082

Innocenzi, V., De Michelis, I., Ferella, F., Beolchini, F., Kopacek, B., Vegliò, F., 2013a. Recovery of yttrium from fluorescent powder of cathode ray tube, CRT : Zn removal by sulphide precipitation. Waste Manag. 33, 2364–2371. doi:10.1016/j.wasman.2013.07.006

Innocenzi, V., De Michelis, I., Ferella, F., Vegliò, F., 2017. Leaching of yttrium from cathode ray tube fluorescent powder: Kinetic study and empirical models. Int. J. Miner. Process. 168, 76–86. doi:10.1016/j.minpro.2017.09.015

Innocenzi, V., De Michelis, I., Ferella, F., Vegliò, F., 2013b. Recovery of yttrium from cathode ray tubes and lamps' fluorescent powders: Experimental results and economic simulation. Waste Manag. 33, 2390–2396. doi:10.1016/j.wasman.2013.06.002

Innocenzi, V., De Michelis, I., Kopacek, B., Vegliò, F., 2014. Yttrium recovery from primary and secondary sources : A review of main hydrometallurgical processes. Waste Manag. 34, 1237–1250. doi:10.1016/j.wasman.2014.02.010

Ippolito, M., De Michelis, I., Medici, F., Innocenzi, V., Vegli, F., 2016. A hydrometallurgical process for the recovery of terbium from fluorescent lamps : Experimental design , optimization of acid leaching process and process analysis. J. Environ. Manage. 184, 552–559. doi:10.1016/j.jenvman.2016.10.026

Ippolito, M., Innocenzi, V., De Michelis, I., Medici, F., Vegli, F., 2017. Rare earth elements recovery from fluorescent lamps : A new thermal pretreatment to improve the efficiency of the hydrometallurgical process. J. Clean. Prod. 153, 287–298. doi:10.1016/j.jclepro.2017.03.195

King, M.J., Davenport, W.G., Moats, M.S., 2013. Chapter 4: Metallurgical offgas cooling and cleaning, in: Matthew J. King, William G. Davenport, M.S.M. (Ed.), Sulfuric Acid

Manufacture (Second Edition). Elsevier Ltd, pp. 31–45. doi:10.1016/B978-0-08-098220-5.00004-6

Lin, E.Y., Rahmawati, A., Ko, J.H., Liu, J.C., 2018. Extraction of yttrium and europium from waste cathode-ray tube (CRT) phosphor by subcritical water. Sep. Purif. Technol. 192, 166–175. doi:10.1016/j.seppur.2017.10.004

Malinowski, C., Malinowska, K., 1994. Oxidation of zinc sulfide by means of zinc sulfate. Thermochim. Acta 246, 141–152.

Meng, W., Wang, X., Yuan, W., Wang, J., Song, G., 2016. The recycling of leaded glass in cathode ray tube (CRT). Procedia Environ. Sci. 31, 954–960. doi:10.1016/j.proenv.2016.02.120

Miskufova, A., Kochmanova, A., Havlik, T., Horvathova, H., Kuruc, P., 2018. Leaching of yttrium, europium and accompanying elements from phosphor coatings. Hydrometallurgy 176, 216–228. doi:10.1016/j.hydromet.2018.01.010

Moezzi, A., Cortie, M., McDonagh, A., 2011. Aqueous pathways for the formation of zinc oxide nanoparticles. Dalt. Trans. 40, 4871. doi:10.1039/c0dt01748e

Moezzi, A., Cortie, M.B., McDonagh, A.M., 2013. Zinc hydroxide sulphate and its transformation to crystalline zinc oxide. Dalt. Trans. 42, 14432. doi:10.1039/c3dt51638e

Murov, S., 2010. Solvent Polarity Table [WWW Document]. URL https://sites.google.com/site/miller00828/in/solvent-polarity-table (accessed 11.2.17).

Okada, T., Yonezawa, S., 2014. Reduction – melting combined with a Na_2CO_3 flux recycling process for lead recovery from cathode ray tube funnel glass. Waste Manag. 34, 1470–1479. doi:10.1016/j.wasman.2014.04.012

Önal, M.A.R., Aktan, E., Borra, C.R., Blanpain, B., Van Gerven, T., Guo, M., 2017a. Recycling

of NdFeB magnets using nitration, calcination and water leaching for REE recovery. Hydrometallurgy 167, 115–123. doi:10.1016/j.hydromet.2016.11.006

Önal, M.A.R., Borra, C.R., Guo, M., Blanpain, B., Van Gerven, T., 2017b. Hydrometallurgical recycling of NdFeB magnets: Complete leaching, iron removal and electrolysis. J. Rare Earths 35, 574–584. doi:10.1016/S1002-0721(17)60950-5

Önal, M.A.R., Borra, C.R., Guo, M., Blanpain, B., Van Gerven, T., 2015. Recycling of NdFeB magnets using sulfation, selective roasting, and water leaching. J. Sustain. Metall. 1, 199–215. doi:10.1007/s40831-015-0021-9

Resende, L. V, Morais, C.A., 2015. Process development for the recovery of europium and yttrium from computer monitor screens. Miner. Eng. 70, 217–221. doi:10.1016/j.mineng.2014.09.016

Resende, L. V, Morais, C.A., 2010. Study of the recovery of rare earth elements from computer monitor scraps – Leaching experiments. Miner. Eng. 23, 277–280. doi:10.1016/j.mineng.2009.12.012

Roy, P., Sardar, A., 2015. SO_2 emission control and finding a way out to produce sulphuric acid from industrial SO2 emission. J. Chem. Eng. Process Technol. 6, 1–7. doi:10.4172/2157-7048.1000230

Singh, N., Wang, J., Li, J., 2016. Waste Cathode Rays Tube: An assessment of global demand for processing. Procedia Environ. Sci. 31, 465–474. doi:10.1016/j.proenv.2016.02.050

Strauss, M.L., Mishra, B., Martins, G.P., 2017. Selective reduction and separation of europium from mixed rare-earth oxides from waste fluorescent lamp phosphors, in: Kim, H., Alam, S., Neelameggham, N.R., Oosterhof, H., Ouchi, T., Guan, X. (Eds.), Rare Metal Technology 2017. The Minerals, Metals & Materials Series. Springer, Cham, pp. 31–36.

doi:10.1007/978-3-319-51085-9

Thorsen, G., Grislingas, A., 1981. Recovery of zinc from zinc ash and flue dusts by hydrometallurgical processing. J. Met. 24–29.

Thorsen, G., Svendsen, F., Grislingas, A., 1984. The integrated organic leaching - solvent extraction operation in hydrometallurgy, in: Bautista, R.G. (Ed.), Hydrometallurgical Process Fundamentals. Springer, Boston, MA, pp. 269–292. doi:10.1007/978-1-4899-2274-8_10

Tian, X., Yin, X., Wu, Y., Tan, Z., Xu, P., 2016. Characterization, recovery potentiality, and evaluation on recycling major metals from waste cathode-ray tube phosphor powder by using sulphuric acid leaching. J. Clean. Prod. 135, 1210–1217. doi:10.1016/j.jclepro.2016.07.044

Tunsu, C., Ekberg, C., Retegan, T., 2014. Characterization and leaching of real fluorescent lamp waste for the recovery of rare earth metals and mercury. Hydrometallurgy 144–145, 91–98. doi:10.1016/j.hydromet.2014.01.019

Tunsu, C., Petranikova, M., Ekberg, C., Retegan, T., 2016. A hydrometallurgical process for the recovery of rare earth elements from fluorescent lamp waste fractions. Sep. Purif. Technol. 161, 172–186. doi:10.1016/j.seppur.2016.01.048

Van Den Bogaert, B., Havaux, D., Binnemans, K., Van Gerven, T., 2015. Photochemical recycling of europium from Eu/Y mixtures in red lamp phosphor waste streams. Green Chem. 17, 2180–2187. doi:10.1039/C4GC02140A

Van Loy, S., Binnemans, K., Van Gerven, T., 2017. Recycling of rare earths from lamp phosphor waste: Enhanced dissolution of $LaPO_4$:Ce^{3+},Tb^{3+} by mechanical activation. J. Clean. Prod. 156, 226–234. doi:10.1016/j.jclepro.2017.03.160

Xu, Q., Yu, M., Kendall, A., He, W., Li, G., Schoenung, J.M., 2013. Environmental and economic evaluation of cathode ray tube (CRT) funnel glass waste management options in the United States. Resour. Conserv. Recycl. 78, 92–104. doi:10.1016/j.resconrec.2013.07.001

Yao, Z., Xie, Z., Tang, J., 2016. A typical e-waste-cathode ray tube glass: Alkaline leaching in the sulfur-containing medium. Procedia Environ. Sci. 31, 880–886. doi:10.1016/j.proenv.2016.02.104

Yin, X., Wu, Y., Tian, X., Yu, J., Zhang, Y., Zuo, T., 2016. Green recovery of rare earths from waste cathode ray tube phosphors : Oxidative leaching and kinetic aspects. ACS Sustain. Chem. Eng. 4, 7080–7089. doi:10.1021/acssuschemeng.6b01965

Yu-Gong, Tian, X., Wu, Y., Zhe-Tan, Lei-Lv, 2016. Recent development of recycling lead from scrap CRTs : A technological review. Waste Manag. 57, 176–186. doi:10.1016/j.wasman.2015.09.004

Zhang, S., Yang, M., Liu, H., 2013. Recovery of waste rare earth fluorescent powders by two steps acid leaching. Rare Met. 32, 609–615. doi:10.1007/s12598-013-0170-6

Zhang, Y., Deng, J., Chen, J., Yu, R., Xing, X., 2014. The electrowinning of zinc from sodium hydroxide solutions. Hydrometallurgy 146, 59–63. doi:https://doi.org/10.1016/j.hydromet.2014.03.006

Highlights

- A new flow sheet is proposed for REEs recovery from CRT powders
- H_2S gas formation and release of toxic elements were avoided by selective roasting
- REEs in the leachate are further purified by oxalate precipitation
- Solvent extraction method with Versatic acid was tested for REE-zinc separation
- Recovery of total zinc is potentially possible by hydrometallurgical methods